LETTERS
PUBLISHED ONLINE: 12 OCTOBER 2015 | DOI: 10.1038/NGEO2557
nature geoscience

Multiple causes of the Younger Dryas cold period

Hans Renssen[1]*, Aurélien Mairesse[2], Hugues Goosse[2], Pierre Mathiot[3], Oliver Heiri[4], Didier M. Roche[1,5], Kerim H. Nisancioglu[6] and Paul J. Valdes[7]

The Younger Dryas cooling event disrupted the overall warming trend in the North Atlantic region during the last deglaciation[1–6]. Climate change during the Younger Dryas was abrupt[7–9], and thus provides insights into the sensitivity of the climate system to perturbations. The sudden Younger Dryas cooling has traditionally been attributed to a shutdown of the Atlantic Meridional Overturning Circulation by meltwater discharges[10–13]. However, alternative explanations such as strong negative radiative forcing[14] and a shift in atmospheric circulation[15] have also been offered. Here we investigate the importance of these different forcings in coupled climate model experiments constrained by data assimilation. We find that the Younger Dryas climate signal as registered in proxy evidence is best simulated using a combination of processes: a weakened Atlantic Meridional Overturning Circulation, moderate negative radiative forcing and an altered atmospheric circulation. We conclude that none of the individual mechanisms alone provide a plausible explanation for the Younger Dryas cold period. We suggest that the triggers for abrupt climate changes such as the Younger Dryas are more complex than suggested so far, and that studies on the response of the climate system to perturbations should account for this complexity.

Proxy data from the North Atlantic region indicate that the Younger Dryas (YD) started 12.9 thousand years ago (ka) with a strong cooling that abruptly terminated the Allerød warm phase[3,4,16]. Summer temperatures in Europe dropped sharply by several degrees[4,16], during a time when the orbitally induced summer insolation at 60° N was close to its 11 ka maximum (that is, 47 W m^{-2} above the modern level[17]). Concurrently, the North Atlantic Ocean experienced a cooling of several degrees[4]. However, the YD cooling was not global, as temperatures in the Southern Hemisphere extratropics were similar to or slightly warmer than during the Allerød time[4,18]. Thus, a mechanism is required that explains all these concurrent features of the YD.

The main hypothesis for the cause of the YD is a catastrophic drainage of Lake Agassiz, leading to freshwater-induced Atlantic Meridional Overturning Circulation (AMOC) collapse and abrupt reduction of the associated northward heat transport[10]. Indeed, model simulations[19] suggest that this mechanism fits very well with several characteristics of the YD, including the abruptness of the YD start, and its characteristic spatial pattern with strongest cooling in the North Atlantic region and relatively warm conditions in Antarctica. However, reconstructions of the AMOC strength do not support a full collapse during the YD (refs 20,21), thus questioning the validity of this hypothesis. In addition, several alternative mechanisms have been proposed for the trigger of the YD. A prominent, but highly debated, hypothesis suggests that the YD was triggered by an extraterrestrial impact[14], leading to enhanced atmospheric dust levels and reduced radiative forcing, possibly in combination with increased ice-sheet melt. Other suggestions include a large solar minimum[22], triggering strong cooling, and a wind shift associated with changes in ice-sheet configuration[15]. Hence, despite decades of intense research, the forcing mechanism of the YD is still debated.

In this study, we analyse different forcing mechanisms for the YD by combining climate model simulations with proxy-based reconstructions, consisting mainly of European July temperatures and North Atlantic annual sea surface temperatures (SSTs; see Supplementary Information). These reconstructions indicate that European summers were on average 1.7 °C cooler than in the

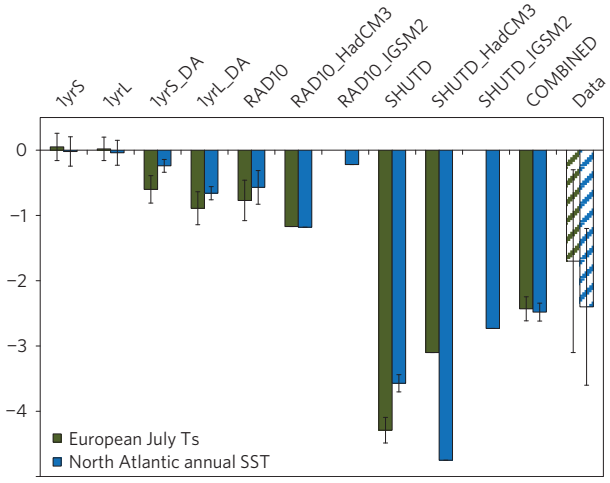

Figure 1 | Simulated temperature anomalies compared to proxy-based estimates (in °C). Simulated European July surface air temperatures (green bars) and annual mean North Atlantic SSTs (blue bars) from various experiments plotted as anomalies relative to the 13 ka reference experiment, compared with proxy-based reconstructions of 12 ka minus 13 ka anomalies (hatched bars). For LOVECLIM results, the ensemble means plus/minus two standard deviations are shown. For proxy-based reconstructions, levels of typical uncertainties are included. Also included are results from HadCM3 and IGSM2 experiments. Domains for Europe and the North Atlantic are 0°–25° E, 40°–70° N and 65°–0° W, 43°–65° N, respectively. For further details, see Table 1 and Supplementary Information.

[1]Department of Earth Sciences, VU University Amsterdam, NL-1081HV Amsterdam, The Netherlands. [2]Earth and Life Institute, Georges Lemaître Centre for Earth and Climate Research, Université catholique de Louvain, B-1348 Louvain-la-Neuve, Belgium. [3]British Antarctic Survey, Natural Environment Research Council, Cambridge CB3 0ET, UK. [4]Institute of Plant Sciences and Oeschger Centre for Climate Change Research, University of Bern, CH–3013 Bern, Switzerland. [5]Laboratoire des Sciences du Climat et de l'Environnement (LSCE), CEA/CNRS-INSU/UVSQ, F-91191 Gif-sur-Yvette Cedex, France. [6]Department of Earth Sciences, University of Bergen and the Bjerknes Centre for Climate Research, N-5020 Bergen, Norway. [7]School of Geographical Sciences, University of Bristol, Bristol BS8 1SS, UK. *e-mail: h.renssen@vu.nl

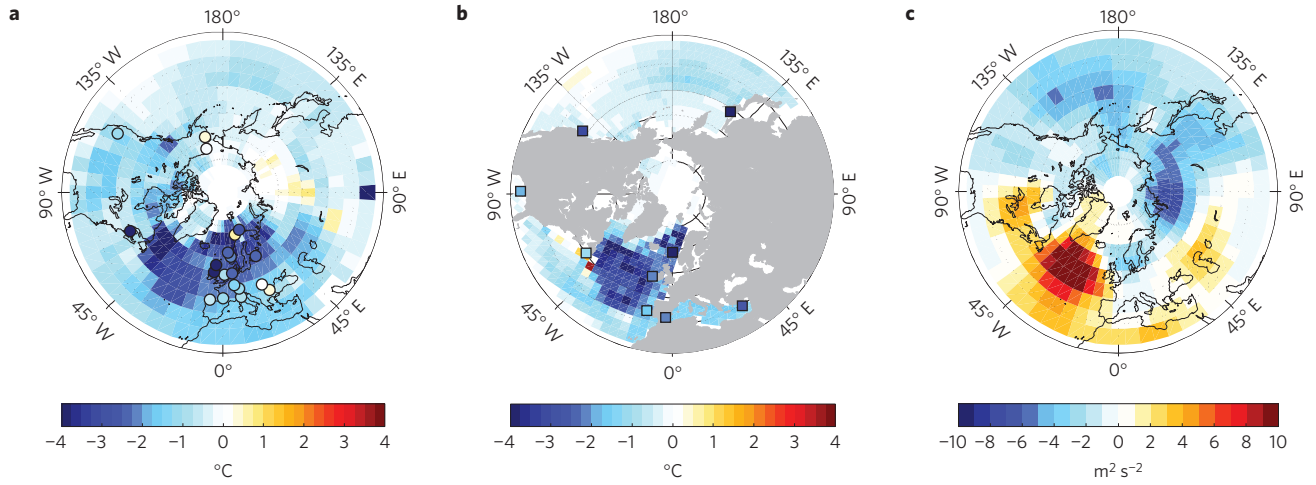

Figure 2 | Simulated anomalies for the COMBINED experiment relative to the 13 ka reference run. a, July surface air temperatures (in °C). **b**, Annual mean SSTs (in °C). **c**, July 800 hPa height (in $m^2\ s^{-2}$). Shown are 100-year ensemble mean values averaged over years 401–500. In our model, the 800 hPa geopotential height (GPH) is considered a better diagnostic for the near-surface atmospheric circulation than sea-level pressure (SLP), as GPH is directly calculated, whereas SLP is derived from other variables. In **a**,**b**, proxy-based estimates (see Supplementary Fig. 1) are included as circles and squares with the same colour scale.

Table 1 | Design of all perturbation experiments.

Experiments	Duration (yr)	Additional FW forcing (Sv)	Radiative forcing ($W\ m^{-2}$)	Ensemble members	Data assimilation
noFW	500	0	0	10	No
1yrS	500	0.5 (1 yr)	0	10	No
1yrL	500	5 (1 yr)	0	10	No
noFW_DA	100	0	0	32	Every 1 yr
1yrS_DA	100	0.5 (1 yr)	0	32	Every 1 yr
1yrL_DA	100	5 (1 yr)	0	96	Every 1 yr
SHUTD	500	4 × Backgr FW	0	10	No
3yrL	100	5 (3 yr)	0	10	No
RAD10	100	0	−10	10	No
3yrLRAD2	100	5 (3 yr)	−2	10	No
COMBINED	1,500	5 (3 yr)	−2	96	Every 5 yr

All experiments were started from a 13 ka reference state (see Supplementary Methods) and were run in ensemble mode. The fifth column indicates the number of ensemble members. The freshwater (FW) pulses were added to the Mackenzie River outlet. All experiments included a representation of the background ice-sheet melt (0.1 Sv in total, see Supplementary Methods), which was removed in COMBINED after 1,000 years. In SHUTD this background flux was multiplied by a factor of 4. The radiative forcing was included as a reduction of the solar constant by 10 $W\ m^{-2}$ (RAD10) or 2 $W\ m^{-2}$ (3yrLRAD2, COMBINED). In COMBINED, an additional random radiative perturbation was applied through the DA (see Supplementary Methods), resulting in a supplementary negative forcing of around −0.17 $W\ m^{-2}$. Further details are provided in the Supplementary Information.

preceding Allerød period at 13 ka (Fig. 1 and Supplementary Fig. 1), with the strongest reduction (up to 4 °C) in NW Europe, diminishing towards the southeast (0.5 °C cooling). The annual SST reconstructions suggest that the North Atlantic was on average 2.4 °C cooler at mid latitudes (Fig. 1 and Supplementary Fig. 1), and further north the cooling was even stronger (−5 °C).

To analyse the possible mechanism for the YD, we performed a set of experiments with the LOVECLIM model in which a 13 ka Allerød reference state was perturbed (Table 1). This reference state was obtained by running the model with persistent appropriate 13 ka background forcings, consisting of orbital parameters, ice sheets, land–sea distribution, and atmospheric trace gas levels. To represent the background melting of the Laurentide and Scandinavian Ice Sheets and to obtain a weaker AMOC considered more realistic for 13 ka conditions, we also applied freshwater fluxes of 0.05 Sv (1 Sv equals $1 \times 10^6\ m^3\ s^{-1}$) in both the NW Atlantic and the Norwegian Sea during the last 500 years of the experiment (see Supplementary Information). This freshwater forcing resulted in local shutdown of Labrador Sea deep convection in agreement with palaeoceanographic evidence[23] and a reduced AMOC strength (from 24 to 16 Sv, Supplementary Fig. 4). All these forcings were maintained in our perturbation experiments.

We constrained part of the simulations by applying a data-assimilation (DA) method (particle filter, see Supplementary Information), enabling us to estimate both the system state and the forcing that are most consistent with the proxy-based YD signal and the model physics. In our evaluation of the model results, we focus on differences between the last 100-year mean of each experiment and the 13 ka reference state (Fig. 1), based on the same variables as provided by the utilized proxy-based reconstructions—that is, North Atlantic annual SSTs, European July air temperatures, and Greenland annual air temperatures.

We first evaluate the impact of short freshwater pulses injected into the Arctic Ocean at the Mackenzie River mouth, in agreement with recent geologic evidence[24] and supported by model studies[25,26] (see Supplementary Discussion). To account for uncertainty, we tested fluxes of 0.5 Sv and 5 Sv, and pulse durations of one and three years (Table 1). Without DA, the 1-year pulses produce no discernible long-term cooling in Europe and the North Atlantic (Fig. 1, experiments 1yrS and 1yrL), and no long-term AMOC weakening. We repeated these simulations with DA using a particle filter applied annually. This generates much stronger cooling in both these areas of interest, ranging from −0.6 to −0.9 °C (Fig. 1, 1yrS_DA and 1yrL_DA). Over Europe, the summer cooling is

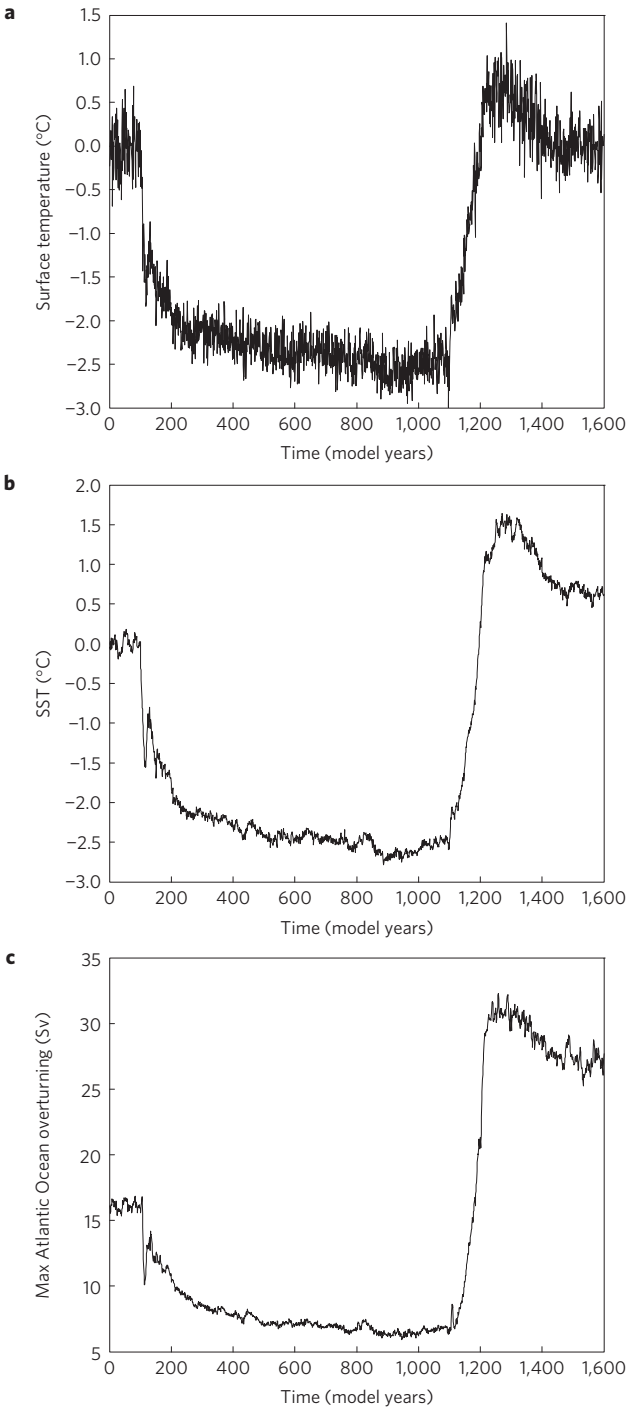

Figure 3 | Simulated time series of key variables. a, European July surface air temperatures (°C). **b**, North Atlantic Annual Mean SSTs (°C). **c**, Maximum strength of the AMOC (in Sv). The results of the first 100 years are derived from our 13 ka reference simulation. The perturbation experiment COMBINED starts in year 101. At year 1101, the background meltwater forcing is removed (see Supplementary Information), leading to a rapid AMOC recovery accompanied by warming of the Atlantic Ocean surface and over Europe. The COMBINED results are ensemble means.

mainly due to anomalous northerly atmospheric flow, transporting cold polar air southwards. This atmospheric shift is associated with reduced surface pressure over Europe and relatively high pressure over the cold North Atlantic that acts as a blocking for westerly flow and for northward heat transport by the atmosphere (Supplementary Fig. 2b,d). A similar pattern is also generated in a simulation with DA, but without any other change in forcings, but is strengthened by the Atlantic Ocean cooling due to freshwater pulses. Nevertheless, the simulated cooling over Europe is still strongly underestimated compared to the proxies (Fig. 1).

We compare this result with two simulations that evaluate alternative mechanisms without data assimilation: AMOC shutdown and negative radiative forcing. In a first experiment (SHUTD), we forced the AMOC to collapse (Supplementary Figs 3 and 4) by quadrupling the background melt fluxes during 500 years. As expected, this generates intense cooling over both the North Atlantic and Europe, on average by more than 3.5 °C (Fig. 1 and Supplementary Fig. 3). However, these temperature reductions clearly exceed the reconstructed cooling over both areas. In the second experiment (RAD10), we prescribed only a strong negative radiative forcing, obtained by reducing the solar constant by 10 W m^{-2}. As anticipated, this causes more widespread cooling than the freshwater-induced AMOC perturbations (Supplementary Fig. 3), but in Europe and the North Atlantic the temperature reduction is comparable to 1yrS_DA and 1yrL_DA (Fig. 1). So, compared to these DA runs with a 1-year freshwater pulse, SHUTD and RAD10 do not improve the model–data temperature match.

A larger negative radiative forcing would generate stronger cooling that could be closer to the proxy-based estimates in the North Atlantic region, but would not match with the relatively mild YD conditions reconstructed in the Southern Hemisphere. Our interpretation is that none of these two mechanisms could be the sole origin of the YD, which is supported by additional experiments performed with different scenarios (see Supplementary Information). Moreover, our model's response in the SHUTD and RAD10 experiments is confirmed by additional simulations performed with two different models (HadCM3 and IGSM2) that show similar temperature anomaly patterns (Supplementary Fig. 8). The sensitivity of LOVECLIM to the perturbations is between that of the other two models (Fig. 1).

Therefore, as a final step, we applied a combined forcing set-up to simulate a climate that is more consistent with proxies (Figs 1 and 2). In this experiment (COMBINED), we employed DA and prescribed both a 3-year, 5 Sv freshwater pulse and a moderate 2 W m^{-2} reduction of the solar constant. In addition, this radiative forcing was randomly perturbed after each DA step, for which a 5-year period was selected. The total radiative perturbation in COMBINED could represent the impacts of the enhanced atmospheric dust load, and reduced atmospheric greenhouse gas concentrations (see Supplementary Information). In COMBINED, we observe considerable changes in the Atlantic Ocean (Fig. 2b), with a southward shift of deep convection, extended Nordic Seas ice cover, and a further AMOC reduction to 7 Sv (Fig. 3c). Over this extended sea-ice cover, air temperatures are 5 to 10 °C lower than in the reference state. In the North Atlantic, the associated SST anomalies closely match reconstructions, as both indicate 2.4 °C cooling (Fig. 1). The simulated atmospheric circulation is similar to the other DA experiments, with anomalous northerly flow over Europe (Fig. 2c). The DA has thus selected anomalous atmospheric conditions that provide the best possible model–data match. This also accounts, to some degree, for possible changes to the forcings not tested with individual perturbation experiments. However, in our set-up, we are unable to assess the contributions of the different forcings to the observed anomalous atmospheric flow. The simulated European cooling of −2.4 °C matches reasonably well with the proxy-based average of −1.7 °C (Figs 1 and 2a). We continued COMBINED in the same set-up for 1,000 years, resulting in a state strongly resembling the YD (Fig. 3a,b). In COMBINED, the particle filter selects and maintains a weakened oceanic state that is most consistent with proxy evidence (Figs 1 and 3), even when the 3-year freshwater pulse has finished. Importantly, this state is not a naturally occurring quasi-equilibrium of the model, and

could be obtained only in experiments with DA that combine the three mechanisms (freshwater pulse, radiative forcing and shift in atmospheric circulation), as other combinations either produced a non-stationary state (Supplementary Fig. 5), or a considerable model–data mismatch (see Supplementary Information). After 1,000 years we removed the background freshwater forcing, resulting in rapid resumption of the Nordic Seas deep convection, and abrupt warming in the North Atlantic region that closely matches the reconstructed YD termination[16] (Fig. 3). However, in reality, the background freshwater forcing probably decreased more gradually during the YD, and the abrupt YD termination resulted from a more complex combination of processes.

The COMBINED results fit very well to proxy-based evidence in Europe and the North Atlantic region with respect to the magnitude, distribution and abruptness of the changes at the start and termination of the YD. The simulated temperature anomalies also agree with proxy-based reconstructions from other regions (Supplementary Fig. 7), and the simulated global cooling of 0.6 °C is fully consistent with independent estimates[4]. On the basis of this good model–data match, we conclude that the YD was most likely caused by a combination of sustained, severe AMOC weakening, anomalous atmospheric northerly flow over Europe, and moderate radiative cooling related to an enhanced atmospheric dust load and/or reduced atmospheric methane and nitrous oxide levels. The exact magnitude of the forcings at the origin of these three processes or potential interactions between them may depend on our experimental design and requires further investigation. Nevertheless, the need for this particular combination of different processes to explain the observed YD cooling pattern is a robust feature of our analysis (see Supplementary Discussion). We regard a full AMOC collapse or any of the other individual mechanisms implausible. The origins of abrupt climate change are thus probably more complex than previously suggested. Our results indicate that the YD occurred only owing to an unusual combination of events, potentially explaining why the YD was different from preceding stadials. This complexity should be accounted for in studies of past abrupt changes and in analyses of the probability of future climate shifts under the influence of anthropogenic forcings.

Methods

Methods and any associated references are available in the online version of the paper.

Received 15 July 2015; accepted 8 September 2015; published online 12 October 2015

References

1. Alley, R. B. *et al.* Abrupt climate change. *Science* **299,** 2005–2010 (2003).
2. Ganopolski, A. & Roche, D. M. On the nature of lead–lag relationships during glacial–interglacial climate transitions. *Quat. Sci. Rev.* **28,** 3361–3378 (2009).
3. Denton, G. H. *et al.* The Last Glacial Termination. *Science* **328,** 1652–1656 (2010).
4. Shakun, J. D. & Carlson, A. E. A global perspective on Last Glacial Maximum to Holocene climate change. *Quat. Sci. Rev.* **29,** 1801–1816 (2010).
5. Clark, P. U. *et al.* Global climate evolution during the last deglaciation. *Proc. Natl Acad. Sci. USA* **109,** E1134–E1142 (2012).
6. Shakun, J. D. *et al.* Global warming preceded by increasing carbon dioxide concentrations during the last deglaciation. *Nature* **484,** 49–54 (2012).
7. Steffensen, J. P. *et al.* High-resolution Greenland ice core data show abrupt climate change happens in few years. *Science* **321,** 680–684 (2008).
8. Brauer, A., Haug, G. H., Dulski, P., Sigman, D. M. & Negendank, J. F. W. An abrupt wind shift in western Europe at the onset of the Younger Dryas cold period. *Nature Geosci.* **1,** 520–523 (2008).
9. Bakke, J. *et al.* Rapid oceanic and atmospheric changes during the Younger Dryas cold period. *Nature Geosci.* **2,** 202–205 (2009).
10. Broecker, W. S., Peteet, D. M. & Rind, D. Does the ocean–atmosphere system have more than one stable mode of operation? *Nature* **315,** 21–26 (1985).
11. Stocker, T. F. & Wright, D. G. Rapid transitions of the ocean's deep circulation induced by changes in the surface water fluxes. *Nature* **351,** 729–732 (1991).
12. Rahmstorf, S. Bifurcations of the Atlantic thermohaline circulation in response to changes in the hydrological cycle. *Nature* **378,** 145–149 (1995).
13. Meissner, K. J. Younger Dryas: A data to model comparison to constrain the strength of the overturning circulation. *Geophys. Res. Lett.* **34,** L21705 (2007).
14. Firestone, R. B. *et al.* Evidence for an extraterrestrial impact 12,900 years ago that contributed to the megafaunal extinctions and the Younger Dryas cooling. *Proc. Natl Acad. Sci. USA* **104,** 16016–16021 (2007).
15. Wunsch, C. Abrupt climate change: An alternative view. *Quat. Res.* **65,** 191–203 (2006).
16. Heiri, O. *et al.* Validation of climate model-inferred regional temperature change for late glacial Europe. *Nature Commun.* **5,** 4914 (2014).
17. Berger, A. & Loutre, M. F. Insolation values for the climate of the last 10 million years. *Quat. Sci. Rev.* **10,** 297–317 (1991).
18. Stenni, B. *et al.* Expression of the bipolar see-saw in Antarctic climate records during the last deglaciation. *Nature Geosci.* **4,** 46–49 (2011).
19. Manabe, S. & Stouffer, R. J. Coupled atmosphere-ocean model response to freshwater input: Comparison to the Younger Dryas event. *Paleoceanography* **12,** 321–336 (1997).
20. McManus, J. F., Francois, R., Gherardi, J. M., Keigwin, L. D. & Brown-Leger, S. Collapse and rapid resumption of Atlantic Meridional Circulation linked to deglacial climate changes. *Nature* **428,** 834–837 (2004).
21. Barker, S. *et al.* Extreme deepening of the Atlantic Overturning Circulation during deglaciation. *Nature Geosci.* **3,** 567–571 (2010).
22. Renssen, H., van Geel, B., van der Plicht, J. & Magny, M. Reduced solar activity as a trigger for the start of the Younger Dryas? *Quat. Int.* **68–71,** 373–383 (2000).
23. Hillaire-Marcel, C., de Vernal, A., Bilodeau, G. & Weaver, A. J. Absence of deep-water formation in the Labrador Sea during the last interglacial period. *Nature* **410,** 1073–1077 (2001).
24. Murton, J. B., Bateman, M. D., Dallimore, S. R., Teller, J. T. & Yang, Z. Identification of Younger Dryas outburst flood path from Lake Agassiz to the Arctic Ocean. *Nature* **464,** 740–743 (2010).
25. Tarasov, L. & Peltier, W. R. Arctic freshwater forcing of the Younger Dryas cold reversal. *Nature* **435,** 662–665 (2005).
26. Condron, A. & Winsor, P. Meltwater routing and the Younger Dryas. *Proc. Natl Acad. Sci. USA* **109,** 19928–19933 (2012).

Acknowledgements

The research leading to these results has received funding from the European Union's Seventh Framework programme (FP7/2007-2013) under grant agreement no. 243908, 'Past4Future. Climate change—Learning from the past climate'. H.R. was supported by a visiting professor grant of the Université catholique de Louvain. H.G. is Senior Research Associate with the Fonds de la Recherche Scientifique (FRS—FNRS-Belgium). D.M.R. is supported by the Netherlands Organization for Scientific Research (NWO) and by the French CNRS.

Author contributions

All authors contributed substantially to this work. H.R. and H.G. conceived the project. H.R., A.M., H.G. and P.M. designed and performed the LOVECLIM experiments. H.R., A.M. and H.G. analysed the model results. O.H. provided proxy-based reconstructions. D.M.R. provided unpublished initial conditions and forcings for the experiments. P.J.V. and K.H.N. performed additional experiments with other models. The manuscript was written by H.R., with input from all other authors.

Additional information

Supplementary information is available in the online version of the paper. Reprints and permissions information is available online at www.nature.com/reprints. Correspondence and requests for materials should be addressed to H.R.

Competing financial interests

The authors declare no competing financial interests.

Methods

We performed the main climate simulations with the LOVECLIM1.2 global climate model[27]. This model has been successfully applied in various palaeoclimatic studies, simulating climates that are consistent with proxy-based climate reconstructions, including the last glacial maximum, the Holocene, the 8.2 ka event and the past millennium[27], showing that LOVECLIM is a valuable tool in palaeoclimate research. It should be noted that this model is of intermediate complexity—however, this makes it possible to perform large ensemble experiments with up to 96 members. Compared with comprehensive general circulation models, the atmospheric module, in particular, has simplified dynamics and low spatial resolution, which limits a detailed representation of the atmospheric circulation. Yet, in the extratropics our model has similar responses to radiative and freshwater forcings as general circulation models and other intermediate complexity models. Further experiments performed with the HadCM3 and IGSM2 models confirm this (see Fig. 1 and Supplementary Fig. 8 and Supplementary information). In several of our simulations we applied a particle filter, which is a data-assimilation method to constrain the model results with proxy-based estimates[28–30]. The proxy-based temperatures employed in this study are based on selected quantitative reconstructions from different sources. Details on the model, the experimental design, the particle filter and the proxy-based temperature reconstructions are provided in the Supplementary Information.

Code availability. The LOVECLIM1.2 code can be accessed at http://www.elic.ucl.ac.be/modx/elic/index.php?id=289.

References

27. Goosse, H. *et al.* Description of the Earth system model of intermediate complexity LOVECLIM version 1.2. *Geosci. Model Dev.* **3,** 603–633 (2010).
28. Dubinkina, S., Goosse, H., Damas-Sallaz, Y., Crespin, E. & Crucifix, M. Testing a particle filter to reconstruct climate changes over the past centuries. *Int. J. Bifurcat. Chaos* **21,** 3611–3618 (2011).
29. Mathiot, P. *et al.* Using data assimilation to investigate the causes of Southern Hemisphere high latitude cooling from 10 to 8 ka BP. *Clim. Past* **9,** 887–901 (2013).
30. Mairesse, A., Goosse, H., Mathiot, P., Wanner, H. & Dubinkina, S. Investigating the consistency between proxy-based reconstructions and climate models using data assimilation: A mid-Holocene case study. *Clim. Past* **9,** 2741–2757 (2013).